



Influence of the ligand donor atoms on the *in vitro* stability of rhenium(I) and technetium (I)-99m complexes with pyrazole-containing chelators: Experimental and DFT studies

Carolina Moura, Célia Fernandes, Lurdes Gano, António Paulo, Isabel C. Santos, Isabel Santos*, Maria José Calhorda

Unidade de Ciências Químicas e Radiofarmacêuticas, ITN, Estrada Nacional 10, 2686-953 Sacavém Codex, Portugal

Departamento de Química e Bioquímica, CQB, Faculdade de Ciências, Universidade de Lisboa, C8, Campo Grande, 1749-016 Lisboa, Portugal

ARTICLE INFO

Article history:

Received 19 September 2008

Received in revised form 4 November 2008

Accepted 5 November 2008

Available online 24 November 2008

Dedicated to Professor Gérard Jaouen on the occasion of his 65th birthday.

Keywords:

Rhenium

Technetium

Carbonyl

Pyrazolyl-containing ligands

DFT calculations

ABSTRACT

The new pyrazole-containing ligand 3,5-Me₂pz(CH₂)₂S(CH₂)₂COOH (**L**¹H) was synthesized and used to prepare the complexes *fac*-[M(κ³-L¹)(CO)₃] (M = Re (**1**), ^{99m}Tc(**1a**)), which were obtained in high yield albeit with a low specific activity in the case of ^{99m}Tc. The X-ray diffraction analysis of **1** confirmed that **L**¹ coordinates to the metal as monoanionic and through a (N,S,O) donor atom set. Challenge experiments of **1a** against cysteine and histidine showed that this complex suffers considerable transchelation *in vitro*. This contrasts with the behavior exhibited by the related complex *fac*-[^{99m}Tc(κ³-L²)(CO)₃] (**2a**) (**L**² = 3,5-Me₂pz-(CH₂)₂NH-CH₂-COO), anchored by a (N₂O)-tridentate ligand. Biodistribution studies of **1a** and **2a** in mice indicated that both compounds have a relatively similar biological profile. Nevertheless, the fastest blood clearance and minor hepatic retention found for **2a** has shown that this complex is more adequate to be further explored in radiopharmaceutical sciences. DFT calculations (ADF program) were performed for these neutral complexes and related cationic M(I) (M = Re, Tc) tricarbonyl complexes anchored by pyrazole-containing ligands, in order to have a better understanding of the influence of the donor atom set (N,N,O vs. N,O,S; N,N,N vs. N,N,S vs. N,S,S) on their *in vitro* stability. The differences of the calculated binding energies are not significant, suggesting that the *in vitro* behavior of these Re(I)/Tc(I) tricarbonyl complexes is not determined by thermodynamic factors.

© 2008 Elsevier B.V. All rights reserved.

1. Introduction

In recent years, the coordination and organometallic chemistry of rhenium and technetium has deserved an increasingly growing interest, reflecting the importance of these d-transition elements in the biomedical field. In fact, technetium-99m still is the most widely used radionuclide for diagnostic imaging in nuclear medicine due to its favorable nuclear properties, low-cost and widespread availability, while rhenium-186 and rhenium-188 are considered useful radionuclides for targeted radiotherapy applications [1]. To obtain medically relevant Re and Tc compounds is necessary to incorporate the metal atom in a coordination complex using an adequate bifunctional ligand. Ideally, the ligand must form a thermodynamically and kinetically stable complex and possess functional groups for further conjugation to a biologically active molecule, somehow related to a certain disease or disease

* Corresponding author. Address: Unidade de Ciências Químicas e Radiofarmacêuticas, ITN, Estrada Nacional 10, 2686-953 Sacavém Codex, Portugal. Tel.: +351 21 9946201; fax: +351 21 9946185.

E-mail address: isantos@itn.pt (I. Santos).

type. In the last decades, a plethora of ^{99m}Tc and ^{186/188}Re complexes presenting different metal cores and having different formal oxidation states (I, III–V) have been investigated aiming at the finding of compounds with increased stability, improved pharmacokinetics and enhanced biological specificity [1–4]. More recently, tricarbonyl Re and Tc complexes emerged as versatile tools in radiopharmaceutical research following the introduction by Alberto and co-workers of the air- and water-stable synthons *fac*-[M(CO)₃(H₂O)₃]⁺ (M = Tc or Re) [5]. So far, the explored chemistry for this synthon has shown a high substitution inertness for the three CO ligands and high substitution lability for the three water molecules. In general, the use of tridentate ligands gives final complexes with highest *in vitro* and *in vivo* stability, and with more favorable and tunable biological properties [6]. Profiting from the versatility offered by these synthons, different research groups have been exploring chelators with several donor atoms, like medium hard tridentate ligands containing nitrogen (i.e. imidazoles, pyrazoles, pyridines), oxygen (i.e. carboxylates), sulfur or phosphorus donor atoms [4–8].

Within this organometallic approach, our research group has introduced and explored pyrazolyl-containing chelators to stabi-

lize the fac - $[M(CO)_3]^+$ ($M = Re, {}^{99m}Tc$) core. In particular, we have evaluated neutral and tridentate chelators, combining a pyrazolyl coordinating group with amino and thioether functions, which were used to prepare several cationic tricarbonyl complexes (**3/3a–6/6a**), as depicted in Chart 1 [8]. By varying the donor atom set (N,N,N vs. N,N,S vs. N,S,S) we intended to evaluate its effect on the kinetics of complexation, as well as on the specific activity, *in vitro/in vivo* stability, pharmacokinetics and biodistribution of the respective tricarbonyl $M(I)$ cations ($M = Re, {}^{99m}Tc$).

Our studies have shown that the ${}^{99m}Tc$ complexes (e.g. **4a**) with pyrazolyl-diamine ligands (N,N,N-donors) are best suited for the design of targeted specific radiopharmaceuticals in comparison with related cations (e.g. **5a**) anchored by pyrazole-dithioether chelators (N,S,S-donors). In fact, the pyrazole-diamine complexes were prepared with higher specific activity, are more resistant to *in vitro* challenge with biologically relevant substrates, like histidine and cysteine, and display a better biological profile in terms of blood clearance, excretory route and overall rate of excretion [9]. The pyrazolyl-diamine chelators have been already applied as bifunctional ligands for labelling a variety of small tumor-seeking peptides with the fac - $[{}^{99m}Tc(CO)_3]^+$ moiety, affording in some cases radiometallated peptides which gave promising pre-clinical results [9].

The encouraging results that have been obtained for the neutral and tridentate pyrazole-containing ligands prompted us to evaluate related classes of ligands having a monoanionic character, expecting to achieve neutral and moderately lipophilic complexes more adequate for the coupling of small non-peptidic biomolecules. To achieve such goal, the coordination capability of the compound [2-(3,5-dimethylpyrazol-1-yl)-ethylamino]acetic acid (**L²H**) towards the fac - $[M(CO)_3]^+$ ($M = Re, {}^{99m}Tc$) moiety was evaluated. This study allowed the synthesis of stable, small and neutral complexes, **2/2a** (see Chart 1), anchored by this monoanionic and (N₂O)-tridentate ligand. These complexes were already coupled to a small biomolecule by conjugation through the central secondary amine. The resulting functionalized Re complex retained the biological activity of the pharmacophore, *i.e.* was still able to inhibit significantly the epidermal growth factor receptor (EGFR) autophosphorylation [10].

Aiming to evaluate the effect of replacing the central amine group of **L²H** by a thioether function on the *in vitro* and *in vivo*

properties of neutral $Re(I)/{}^{99m}Tc(I)$ tricarbonyl complexes anchored by pyrazole-containing chelators, we have extended our investigation to the congener ligand [2-(3,5-dimethylpyrazol-1-yl)-ethylthio]-acetic acid (**L¹H**). In this work, we report on the synthesis and characterization of this novel chelator (**L¹H**), and on the corresponding tricarbonyl complexes fac - $[M(\kappa^3-L^1)(CO)_3]$ ($M = Re$ (**1**), ${}^{99m}Tc$ (**1a**)) (Chart 1). For both **1a** and the congener fac - $[{}^{99m}Tc(\kappa^3-L^2)(CO)_3]$ (**2a**), the *in vitro* stability in challenge experiments against cysteine and histidine will be also presented, as well as the evaluation of their *in vivo* stability and biodistribution in mice. Searching for a better understanding of the influence of the ligand donor atom set on the *in vitro* stability of neutral and cationic $Re(I)$ and ${}^{99m}Tc(I)$ tricarbonyl complexes anchored by pyrazolyl-containing chelators, DFT (density functional theory) calculations [11] have been performed for compounds **1/1a–6/6a** (Chart 1), and will be also discussed herein.

2. Results and discussion

2.1. Synthesis and characterization of **L¹H** and its $Re(I)$ and ${}^{99m}Tc(I)$ tricarbonyl complexes

As shown in Scheme 1, the new pyrazole-containing ligand, [2-(3,5-dimethylpyrazol-1-yl)-ethylthio]-acetic acid (**L¹H**), was prepared by *S*-alkylation of mercaptoacetic acid with *N*-(2-bromoethyl)-3,5-dimethylpyrazole. **L¹H** was obtained as a white solid with an almost quantitative isolated yield (98%), after adequate work-up. The formulation proposed for **L¹H** was corroborated by elemental analysis, IR, ¹H and ¹³C NMR spectroscopy.

The reaction of the starting material fac - $[Re(H_2O)_3(CO)_3]Br$ [12] with **L¹H** in refluxing water yielded fac - $[Re(\kappa^3-L^1)(CO)_3]$ (**1**), which precipitated from the reaction mixture (Scheme 1). Compound **1** was recovered in moderate yield (60%) as a microcrystalline white solid, and is stable towards aerial oxidation or hydrolysis either in the solid state or in solution. The characterization of **1** involved the common spectroscopic techniques (IR, ¹H and ¹³C NMR) and X-ray diffraction analysis.

The most significant feature of the IR spectrum of **1** is the presence of a set of four intense bands in the range 2027–1879 cm^{-1} that were easily assigned to the $\nu(C\equiv O)$ stretching modes. There is also an intense band at 1644 cm^{-1} due to $\nu(C=O)$ of the terminal

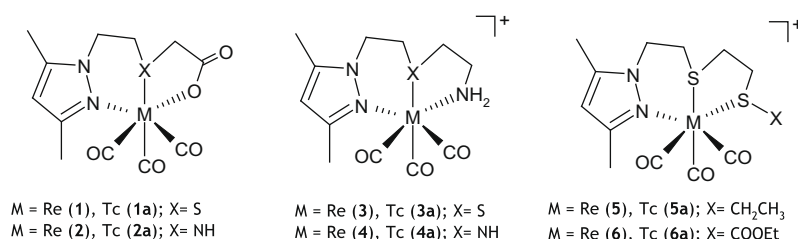
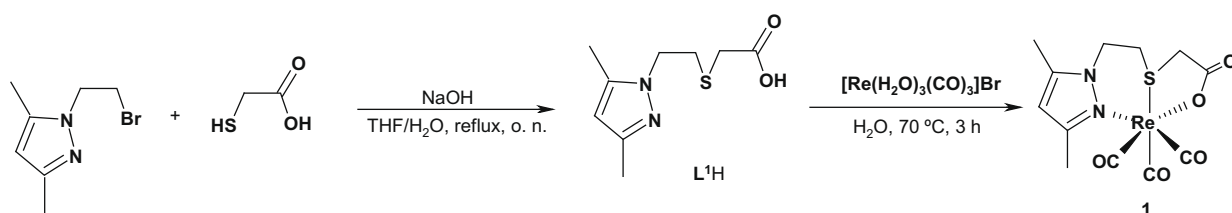


Chart 1. Cationic (**1/1a** and **2/2a**) and neutral (**3/3a–6/6a**) Re and Tc tricarbonyl complexes with the pyrazole-containing chelators addressed in this work.



Scheme 1. Synthesis of **L¹H** and fac - $[Re(\kappa^3-L^1)(CO)_3]$ (**1**).

carboxylate group. This frequency is red shifted ($\Delta\nu = 64 \text{ cm}^{-1}$) relatively to the frequency of the same band in free **L¹H** which confirms that the carboxylate from **L¹** is coordinated to the metal.

The ¹H NMR spectrum of **1** showed a set of six CH₂ resonances, between 2.60 and 4.75 ppm, integrating for one proton each. They indicate the presence of diastereotopic methylenic protons as a consequence of the facial coordination of **L¹** through the carboxylate, the central sulfur atom and the pyrazolyl ring. This coordination mode was confirmed by the X-ray diffraction analysis of **1** (Fig. 1). Table 1 summarizes selected bond distances and angles found for **1**, as well as those obtained from DFT optimization of this complex (see below). In the structure of **1**, the rhenium atom is six-coordinate with a distorted octahedral coordination geometry, as can be seen from the angles around the rhenium atom which vary between 86.17(13) and 99.11(13)°. The values of the Re–C (1.897(3)–1.914(3) Å), Re–S (2.4858(7) Å), Re–O (2.1219(19) Å) and Re–N (2.203(2) Å) bond distances are comparable to those reported for other octahedral complexes containing the *fac*-[Re(CO)₃]⁺ unit and the same donor atoms [7,8,10].

The congener radioactive complex *fac*-[^{99m}Tc(CO)₃(κ³-L¹)]⁺ (**1a**) was obtained with almost quantitative yield (>99%) by reaction of *fac*-[^{99m}Tc(H₂O)₃(CO)₃]⁺ with **L¹H** in phosphate buffer (pH 7.4) at 100 °C during 1 h (Scheme 2). The identity of complex **1a** was

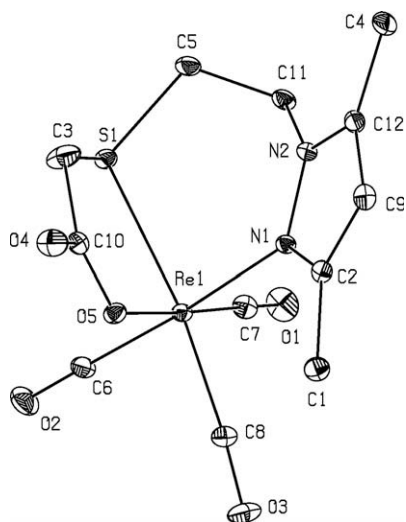
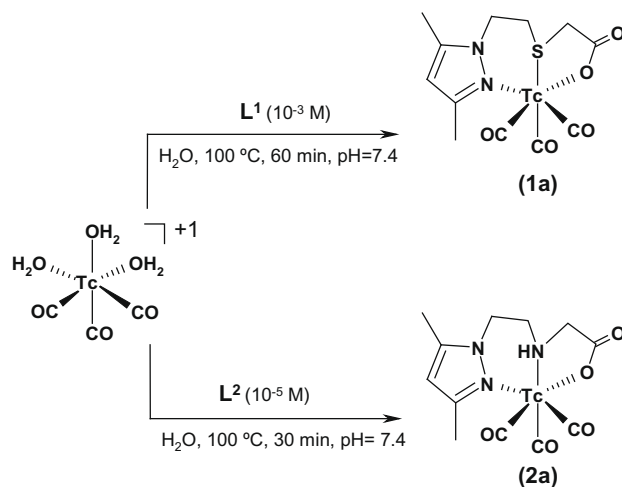


Fig. 1. ORTEP view of complex **1**. Vibrational ellipsoids are drawn at the 40% probability level.

Table 1
Selected bond lengths (Å) and angles (°) from DFT calculations (in gas phase and in the presence of methanol) for [M(CO)₃{3,5-Me₂pz-(CH₂)₂S-CH₂-COO}] (M = Re, **1**; Tc, **1a**), and comparison with the X-ray structural data of complex **1**.

Parameter	Complex 1			Complex 1a	
	DFT data (gas phase)	DFT data (MeOH)	X-ray	DFT data (gas phase)	DFT data (MeOH)
M1–C7	1.908	1.909	1.897(3)	1.905	1.901
M1–C8	1.916	1.917	1.908(3)	1.913	1.915
M1–C6	1.912	1.914	1.914(3)	1.908	1.905
M1–O5	2.128	2.143	2.1219(19)	2.125	2.153
M1–S1	2.514	2.517	2.4858(7)	2.516	2.517
M1–N1	2.241	2.228	2.203(2)	2.245	2.237
C8–M1–C6	88.22	88.28	86.16(13)	88.30	88.03
C8–M1–C7	87.22	87.24	89.31(14)	87.26	86.86
C6–M1–C7	87.53	87.78	88.77(14)	87.65	87.81
C8–M1–N1	95.69	95.91	96.42(11)	95.67	95.84
C7–M1–N1	96.79	96.61	96.48(11)	96.67	96.29
C7–M1–S1	98.27	98.38	99.11(9)	98.23	98.42
C6–M1–S1	89.98	89.91	89.81(9)	89.93	90.26



Scheme 2. Synthesis of complexes *fac*-[^{99m}Tc(CO)₃(κ³-L)(CO)₃] (L = L¹ (**1**), L² (**2**)).

established by comparing its HPLC radiochromatograms with the UV–Vis trace of the Re surrogate (complex **1**).

The synthesis of **1a** required the use of a 10^{−3} M concentration of **L¹H** to increase the kinetics of the reaction and to avoid some oxidation to ^{99m}TcO₄[−], in contrast with the behavior exhibited by the congener **L²H** (Scheme 2) [10]. The same trend was already observed during the synthesis of the related cationic ^{99m}Tc tricarbonyl complexes, **3a–6a** (see Chart 1), *i.e.* the successive replacement of an amino group by thioethers led to chelators which have to be used in highest concentration to assure a complete reaction with the aqua-tricarbonyl precursor [8b].

Compound **1a** has a log*D* = 1.26 ± 0.04 [13], a value which is higher than the one found for **2a** (log*D* = 1.10 ± 0.03), reflecting the influence of the central donor group (S vs. NH) on the lipophilicity of these complexes.

In a comparative way, we have studied the resistance of complexes **1a** and **2a** against transchelation, using a 10³-fold excess of two potentially metal-binding amino acids, cysteine and histidine. Complex **2a** does not undergo significant transchelation with cysteine or histidine, even after 24 h of incubation at 37 °C. By contrast, after 6 h of incubation roughly 50% of complex **1a** already reacted with these aminoacids, affording the respective ^{99m}Tc(I) tricarbonyl complexes (Fig. 2).

These results showed that the donor atom set (N,N,O vs. N,S,O) can have a dramatic influence on the *in vitro* stability of neutral ^{99m}Tc(I) tricarbonyl complexes against challenge with cysteine

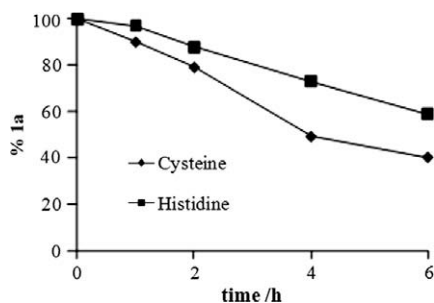


Fig. 2. Stability of complex **1a** in the presence of histidine and cysteine ([amino acid]/[L¹H] = 100).

and histidine. The same trend was observed for related cationic complexes (**3a–6a**), but in this case the influence of the nature of the donor atoms was less significant [8b,9a].

2.2. Biodistribution studies

Biodistribution studies of **1a** and **2a** were performed in female CD-1 mice, in order to evaluate the influence of the central donor group (secondary amine vs. thioether) on the *in vivo* behavior of the complexes. The biological profiles found for **1a** and **2a** are similar and reflect the lipophilic character of both complexes. Complex **2a** shows the fastest blood clearance, with blood activities of 1.2 ± 0.1 and $0.37 \pm 0.08\%$ ID/g at 1 h and 4 h p.i., respectively. Complex **1a** is more retained in the blood stream ($1.6 \pm 0.3\%$ ID/g, 1 h p.i.; $1.5 \pm 0.2\%$ ID/g, 4 h p.i.) although its blood clearance can still be considered relatively fast. Only a negligible fraction of the injected radioactivity was found in the stomach (values between 0.5 and 0.9% ID/g), demonstrating that **1a** and **2a** are not undergoing *in vivo* reoxidation to $^{99m}\text{TcO}_4^-$, a species which is taken by this organ. In agreement with their lipophilic character, both complexes have high liver uptake especially **1a** (**1a**: $35.1 \pm 8.3\%$ ID/g (1 h p.i.), $28.3 \pm 3.0\%$ ID/g (4 h p.i.); **2a**: $13.0 \pm 3.0\%$ ID/g (1 h p.i.), $7.3 \pm 2.3\%$ ID/g (4 h p.i.)). The accumulation of the radioactivity in the intestines suggests the hepatobiliary tract as the predominant

excretory route (**1a**, $4.9 \pm 0.8\%$ ID/g (1 h p.i.), $5.1 \pm 0.4\%$ ID/g (4 h p.i.); **2a**: $18.2 \pm 2.4\%$ ID/g (1 h p.i.), $18.6 \pm 3.2\%$ ID/g (4 h p.i.)), the excretion of **1a** being slower than that of **2a**. The whole animal body excretion rate, either by the hepatobiliary or urinary pathways, is relatively slow for both complexes (**1a**: $9.8 \pm 6.8\%$ ID (1 h p.i.), $35.8 \pm 2.2\%$ ID (4 h p.i.); **2a**: $24.5 \pm 1.6\%$ ID (1 h p.i.), $29.7 \pm 3.5\%$ ID (4 h p.i.)).

The metabolic stability of complexes **1a** and **2a** has been assessed by HPLC analysis of the urine and blood of mice injected with these complexes. These studies have shown that the intact complexes correspond to the major part of the circulating activity. However, a significant amount of metabolites were detected in the urine, as can be seen in the radiochromatograms presented in Fig. 3. The occurrence of metabolization is most probably related with the biological elimination of the compounds and seems to be more extensive for **1a**, as a larger proportion of metabolites were detected in the urine of the mice injected with this complex. It is not clear whether this behavior is related or not with the greatest reactivity towards biologically relevant substrates observed for **1a** *in vitro*.

2.3. Computational studies

DFT calculations on Tc and Re complexes potentially relevant in the radiopharmaceutical field, namely organometallic derivatives of $\text{fac-}[M(\text{CO})_3]^+$ ($M = \text{Re}, \text{Tc}$), were recently reported [14–16]. Geerling et al. investigated the influence of different combinations of N, O and S donor atoms ligands on the stability of Re(I)/Tc(I) tricarbonyl complexes, using simplified models of the real compounds [16].

In this work, DFT calculations [11] (see Section 4.9) were carried out on Re/Tc complexes **1/1a–6/6a** (Chart 1) with pyrazole-containing chelators with different donor atoms [8,10], in order to rationalize the *in vitro* stability of the complexes.

The geometry of complexes **1/1a–6/6a** and the isolated ligands, modeled after the available experimental X-ray structures of compounds **1–4** and **6**, was optimized without any symmetry constraints, both in the gas phase and in the presence of solvent (methanol), using the COSMO method [17]. The agreement

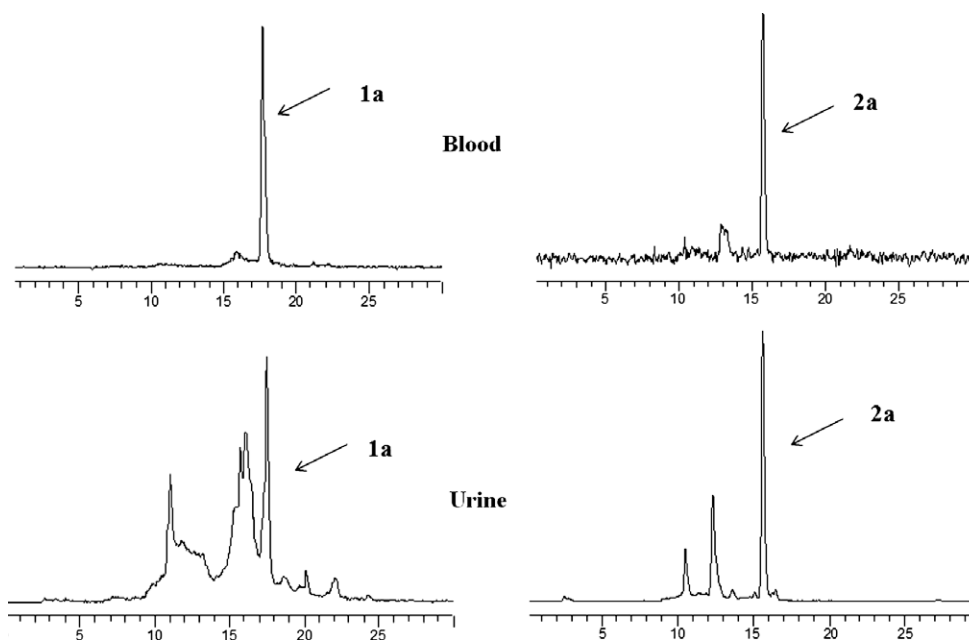


Fig. 3. HPLC analysis (radiometric detection) of urine and blood from mice administered with **1a** or **2a** at 1 h p.i.

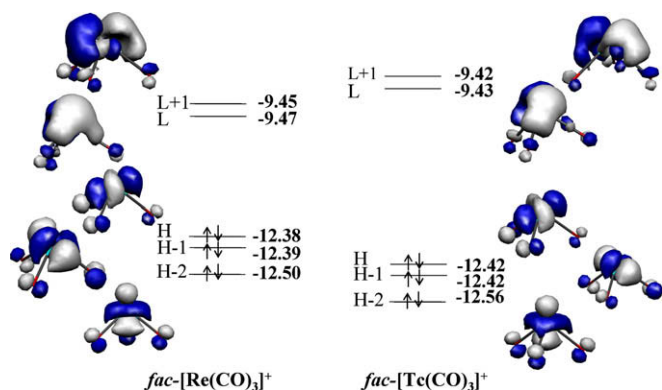


Fig. 4. The frontier orbitals of the *fac*-[M(CO)₃]⁺ (M = Re, Tc) fragments (energies in eV).

between calculated and experimental structures (when available) is quite good, and the effect of the solvent on bond distances and angles is negligible, as can be seen in Table 1 and in Supplementary material for complexes [M(CO)₃{3,5-Me₂pz-(CH₂)₂S-CH₂-COO}] (M=Re, **1**; Tc, **1a**). No significant differences are observed between the bond lengths and angles calculated for the corresponding complexes of Re and Tc.

The frontier orbitals of facial d⁶ [M(CO)₃]⁺ (M = Re, Tc) are displayed in Fig. 4 and are typical of the conical C_{3v} ML₃ fragments [18]. The three lower levels are derived from the octahedron t_{2g} set, while the two empty higher levels derive from the octahedron e_g set. The HOMO–LUMO gap is larger for [Tc(CO)₃]⁺ than in the Re analogue, indicating that, according to the HSAB theory, this fragment is harder [19].

The energies of the HOMO and LUMO of the isolated pyrazole-containing ligands used to prepare complexes **1/1a–6/6a** are shown in Fig. 5. The LUMO of all ligands, except 3,5-Me₂pz(CH₂)₂S(CH₂)₂SCH₂COOEt (complexes **6/6a**) is a π orbital of the pyrazole ring, which can thus behave as an acceptor. In 3,5-

Me₂pz(CH₂)₂S(CH₂)₂SCH₂COOEt, it is mostly localized in the COO group. The HOMOs are localized in different donor atoms of each ligand: in the carboxylate, when it is present, in the two nitrogen atoms in Me₂pz(CH₂)₂NH(CH₂)₂NH₂, and in the sulfur (the terminal one, when there are two S atoms) in the others. The HOMOs of the anionic ligands display the highest energy (by ~4 eV), and they can therefore be considered softer than the neutral ligands (see also Supplementary material). The differences in energy between HOMOs of the neutral ligands are very small, but the ligands containing sulfur donor atoms tend to be softer than the one containing NH, with the exception of [3,5-Me₂pz-(CH₂)₂S-(CH₂)₂-SCH₂COOEt], owing to the presence of the ester function. Indeed, sulfur is softer than nitrogen accordingly to Pearson's hard-soft classification of acids and bases [19]. However, the inverse trend was seen in the monoanionic ligands with L¹ (N,S,O) having a lower energy HOMO than L² (N,N,O), showing that such a simple mode cannot be used.

The binding energy (ΔE) of complexes **1/1a–6/6a** sequence, calculated as the difference between the energy of complex with the optimized geometry (E_{complex}) and the sum of energies of the optimized ligands (E_{ligand}) and fragments *fac*-[M(CO)₃]⁺ (M = Re, Tc; $E_{[\text{M}(\text{CO})_3]^+}$) (Eq. (1)), was used to analyze their stability

$$\Delta E = E_{\text{complex}} - (E_{\text{ligand}} + E_{[\text{M}(\text{CO})_3]^+}) \quad (1)$$

The interaction energy ($\Delta E'$) between fragments can be decomposed in three terms $\Delta E_{\text{Pauli}} + \Delta E_{\text{elec}} + \Delta E_{\text{orb}}$ (see Section 4.9). The binding energy ΔE can be obtained from $\Delta E'$, by adding the reorganization energies of the fragments (difference between the energy of each fragment with the geometry it adopts in the complex and the energy of the optimized structure). These values were calculated in the gas phase and are given in Table 2, as well as the binding energies in methanol.

In the gas phase, the neutral complexes (**1/1a** and **2/2a**) are more stable than the cationic ones (**3/3a–6/6a**) by approximately 100 kcal/mol, as can be seen in Table 2 and Fig. 6A, and the Re complexes (**1–6**) are more stable than the corresponding Tc complexes (**1a–6a**) by ~15–18 kcal/mol. The energy decomposition terms (Table 2) suggest that the interaction energy $\Delta E'$ almost reflects the

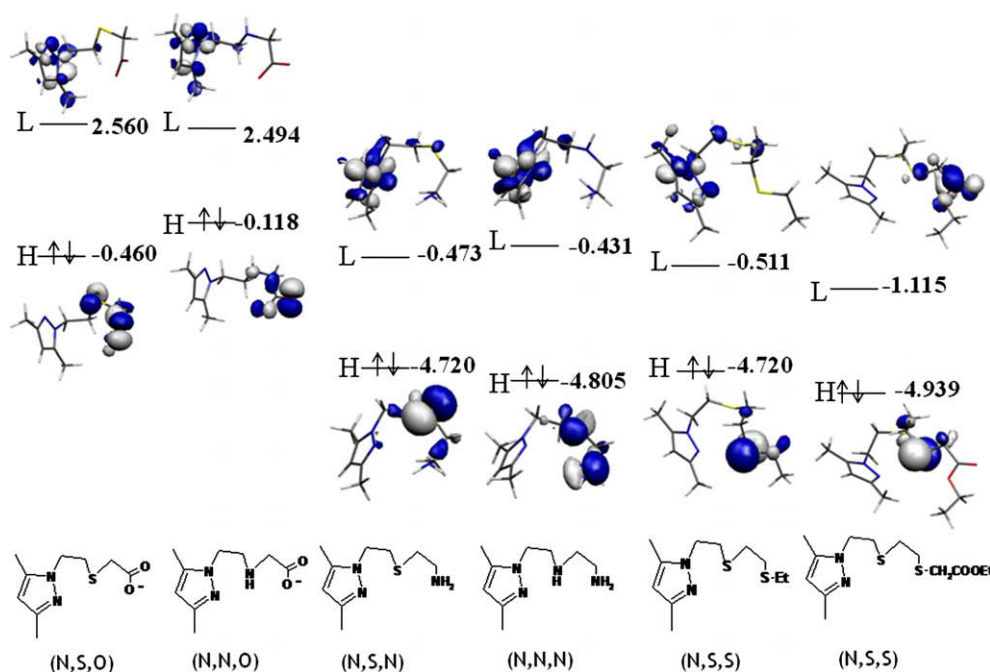
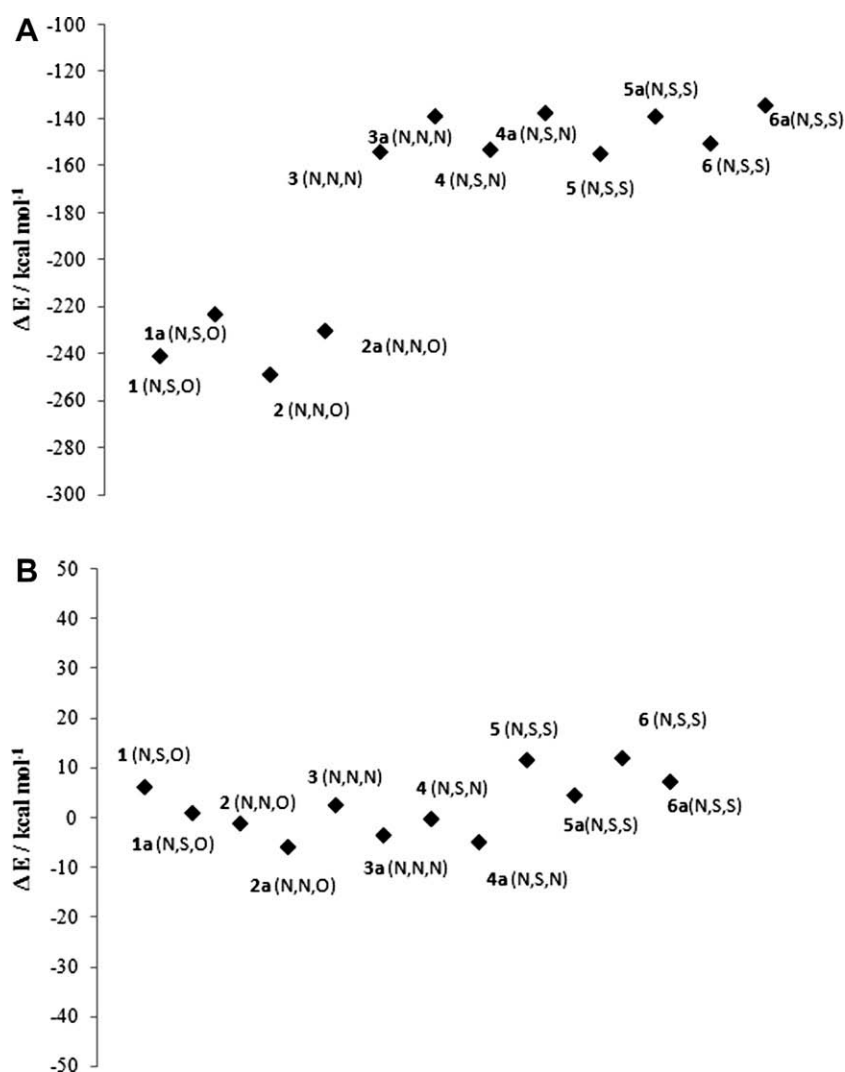


Fig. 5. The HOMOs (H) and LUMOs (L) of the ancillary ligands of complexes **1/1a–6/6a** (energies in eV).

Table 2Energy decomposition analysis for complexes **1/1a–6/6a** in the $[\text{M}(\text{CO})_3]^+$ ($\text{M} = \text{Re}, \text{Tc}$) fragment and the ligand (energies in kcal mol^{-1}).

Complexes	1/1a		2/2a		3/3a		4/4a		5/5a		6/6a	
	N,S,O		N,N,O		N,S,N		N,N,N		N,S,S		N,S,S	
	Re	Tc										
ΔE_{Pauli}	188.83	152.99	195.12	159.29	186.65	153.36	188.61	150.77	182.22	149.32	181.36	146.56
ΔE_{elec}	-278.63	-246.04	-297.74	-263.55	-194.49	-164.86	-208.51	-174.42	-178.38	-150.09	-175.07	-145.41
ΔE_{orb}	-172.46	-149.90	-173.02	-151.19	-157.59	-136.97	-153.12	-131.67	-166.85	-144.92	-166.98	-144.05
$\Delta E'$	-262.27	-242.96	-275.64	-255.44	-165.43	-148.48	-173.02	-155.32	-163.01	-145.69	-160.69	-142.90
ΔE_{reorg}	21.60	19.98	27.13	25.44	11.24	9.37	19.74	17.59	8.02	6.47	10.04	8.37
ΔE	-240.67	-222.98	-248.51	-230.00	-154.19	-139.11	-153.28	-137.73	-154.99	-139.22	-150.65	-134.53
ΔE (MeOH)	6.15	0.94	-1.18	-5.9	2.51	-3.54	-0.27	-4.92	11.58	4.48	11.96	7.21

**Fig. 6.** Binding energy in the gas phase (A) and in the presence of methanol (B) for complexes **1/1a–6/6a**.

ΔE_{elec} term, with the Pauli repulsion and the orbital interaction (ΔE_{Pauli} and ΔE_{orb}) practically canceling each other. The ΔE_{elec} term is much higher for the carboxylate containing anionic ligands. The Pauli repulsion is significantly larger for Re than for Tc, as the 5d orbitals are much more diffuse. The same fact probably explains the larger covalent interaction taking place between the $[\text{Re}(\text{CO})_3]^+$ fragment and the ligands, compared with the analogous Tc fragment. The reorganization energies are substantially higher for the ligands than for the conical $[\text{M}(\text{CO})_3]^+$ ($\text{M} = \text{Re}, \text{Tc}$) fragments (about 2–3 kcal mol^{-1} for these). The anionic ligands require the

highest energy to adopt the geometry they have in the complexes, with the maximum for the N containing ligand. The large differences between complexes are not realistic and the binding energies ΔE were recalculated taking into account the solvent (methanol). The new $\Delta E(\text{MeOH})$ values are almost identical for both the neutral and cationic complexes (Table 2 and Fig. 6B). The highest solvation energy of the $[\text{Re}(\text{CO})_3]^+$ fragment (-303.65 kcal/mol) compared with $[\text{Tc}(\text{CO})_3]^+$ (-258.08 kcal/mol) contributes to make the binding energies for Re and Tc complexes much closer.

The successive replacement of nitrogen by sulfur donor atoms results, both in the gas phase and in methanol, in less stable compounds by approximately 4–10 kcal/mol, for the neutral (**1/1a** and **2/2a**) and cationic (**3/3a–6/6a**) tricarbonyl complexes. The same trend was found by other authors, who have applied DFT calculations to a series of model complexes containing the *fac*-[M(CO)₃]⁺ (M = Re, Tc) cores, and have reported differences on energies in the range of 20–30 kcal/mole upon replacement of two or three N donor atoms by sulfur [16]. The much smaller energy differences found in this work are probably associated with having used the tridentate ligands themselves, rather than a small model as the other authors did in their DFT calculations.

3. Conclusions

The novel pyrazolyl-containing ligand **L¹H** forms well defined tricarbonyl complexes, *fac*-[M(κ^3 -**L¹**)(CO)₃] (M = Re (**1**), ^{99m}Tc (**1a**)), both at macroscopic (Re) and no-carrier-added level (^{99m}Tc). The characterization of the Re complex by the common spectroscopic techniques confirmed that **L¹** acts as a tridentate and monoanionic ligand, a coordination mode that we have found previously for the congener ligand (**L²**) containing a central amine function instead of a central thioether.

A comparative study of the complexes *fac*-[^{99m}Tc(κ^3 -**L**)(CO)₃] (L = **L¹** (**1a**), **L²** (**2a**)) has shown that the nature of the ancillary ligand has a strong influence on their *in vitro* stability against transchelation with metal-binding aminoacids (cysteine and histidine), and it was observed that the introduction of the thioether group clearly enhances the reactivity of the compounds towards these aminoacids. In spite of these differences, the evaluation of the bio-distribution of **1a** and **2a** in mice has shown that the compounds have a relatively similar profile. In particular, both complexes seem to undergo metabolization processes, as several metabolites have been detected in the urine of mice injected with **1a** and **2a**. The occurrence of metabolization is not necessarily a negative aspect in what concerns the use of these complexes in the design of radiopharmaceuticals since it may accelerate the elimination of the compounds and, therefore, increase the clearance from non-target tissues. Nevertheless, the less pronounced hepatic retention observed for **2a** indicates that this complex is more promising to be further explored in radiopharmaceutical research. A similar tendency has been previously observed by our research group for related cationic complexes, i.e. the inclusion of thioether coordinating groups enhances the liver uptake of the complexes, most probably as a consequence of their increasing lipophilicity.

DFT calculations were performed for the neutral (**1/1a** and **2/2a**) and cationic (**3/3a–6/6a**) complexes anchored by pyrazole-containing chelators, in order to have a more rationale insight into the influence of different donor atom sets on the *in vitro* stability of the complexes. This study has shown that the replacement of nitrogen by sulfur donor atoms led to slightly less stable complexes ($\Delta E \sim 4$ –10 kcal/mol). However, these differences are not significant enough to explain the lower *in vitro* stability observed experimentally for the complexes with the ligands containing sulfur donor atoms, suggesting that the *in vitro* behavior of these complexes is not controlled by thermodynamic factors. A more complete study of the reaction mechanism for the formation of the complexes, taking into account the most stable intermediates and likely transition states, is being performed, in order to determine energy barriers for each kind of ligand.

4. Experimental

The synthesis of the ligands and complexes were carried under a nitrogen atmosphere, using standard Schlenk techniques and dry

solvents, while the work-up procedures were performed under air. The compound *N*-(2-bromoethyl)pyrazole [20] was prepared according to published methods. The starting material *fac*-[Re-(H₂O)₃(CO)₃]Br [12] was synthesized by the literature method. Na[^{99m}TcO₄] was eluted from a commercial ⁹⁹Mo/^{99m}Tc generator, using 0.9% saline. Complex **2a** was prepared as previously reported.[10] ¹H and ¹³C NMR spectra were recorded on a Varian Unity 300 MHz spectrometer; ¹H and ¹³C chemical shifts are given in ppm and were referenced with the residual solvent resonances relative to SiMe₄. IR spectra were recorded as KBr pellets on a Bruker, Tensor 27 spectrometer. C, H and N analyses were performed on an EA 110 CE Instruments automatic analyser. Thin layer chromatography (TLC) was done using plates from Merck (silica gel 60 F254). Column chromatography was performed in silica gel 60 (Merck). HPLC analysis was performed on a Perkin-Elmer LC pump 200 coupled to a LC 290 tunable UV-Vis detector and to a Berthold LB-507A radiometric detector, using a Macherey-Nagel C18 reversed-phase column (Nucleosil 10 μ m, 250 \times 4 mm) and a gradient of aqueous 0.1% CF₃COOH (A) and methanol (B) with a flow rate of 1.0 mL min⁻¹. Method: 0–3 min, 100% A; 3–3.1 min, 100% \rightarrow 75% A; 3.1–9 min, 75% A; 9–9.1 min 75% \rightarrow 66% A; 9.1–20 min, 66% \rightarrow 0% A; 20–25 min, 0% A; 25–25.1 min, 0% \rightarrow 100% A; 25.1–30 min, 100% A.

4.1. Synthesis of [2-(2-(3,5-dimethyl-pyrazol-1-yl)ethylthio)]acetic acid (**L¹H**)

To a solution of mercaptoacetic acid (167 μ L, 2.45 mmol) in H₂O (7 mL) was added NaOH (196 mg; 4.90 mmol) and the reaction mixture was refluxed for 15 min. After cooling to room temperature, a solution of 1-(2-bromoethyl)pyrazole (500 mg, 2.45 mmol) in THF (7 mL) was added dropwise to the mixture. After overnight reflux, the solvent was removed under vacuum. The residue obtained was applied on the top of a silica-gel column which was eluted with CHCl₃/MeOH/NH₄OH (70/28/2). The removal of the solvent from the collected fractions gave compound **L¹H** as a white microcrystalline solid. Further purification of **L¹H** was done by dissolution of the compound in distilled water followed by precipitation as the free carboxylic acid by adjustment at pH 1 with 2 N HCl. Yield: 98% (514 mg, 2.40 mmol).

Anal. Calc. for C₉H₁₄N₂O₂S.H₂O: C, 46.53; H, 6.94; N, 12.06. Found: C, 46.00; H, 7.00; N, 12.62%. IR (KBr, ν /cm⁻¹): 1581 (s) ν (C=O). ¹H NMR (CD₃OD): δ 2.13 (3H, s, CH₃-pz), 2.27 (3H, s, CH₃-pz), 2.92 (2H, t, CH₂-S), 3.09 (2H, s, CH₂-COOH), 4.17 (2H, t, pz-CH₂), 5.79 (1H, s, H(4)). ¹³C NMR (CD₃OD): δ 11.2 (CH₃-pz), 13.3 (CH₃-pz), 33.5 (CH₂); 38.1 (CH₂), 48.0 (CH₂), 105.9 (C(4)-pz), 141.6 (C(3/5)-pz), 148.9 (C(3/5)-pz), 177.7 (C=O). R_f (silica-gel, CHCl₃/MeOH/NH₄OH (70/28/2)) = 0.50.

4.2. Synthesis of *fac*-[Re(κ^3 -**L¹**)(CO)₃] (**1**)

To an aqueous solution (10 mL) of *fac*-[Re(CO)₃(H₂O)₃]Br (50 mg, 0.24 mmol) was added an equimolar amount of **L¹H** (33 mg, 0.40 mmol) dissolved in H₂O (10 mL). The resulting solution was heated at 70 °C for 3 h. After cooling to room temperature, complex **1** precipitated as a white microcrystalline solid which was separated by filtration and dried under vacuum. Yield: 60% (36 mg, 0.07 mmol).

Anal. Calc. for ReC₁₂H₁₃N₂O₅S.H₂O: C, 28.74; H, 3.01; N, 5.59. Found: C, 28.62; H, 2.67; N, 4.51%. IR (KBr, ν /cm⁻¹): 1644 (s) ν (C=O), 1879 (s) ν (C=O); 1934 (s) ν (C=O); 2027 (s) ν (C=O). ¹H NMR (CD₃OD): δ 2.37 (3H, s, CH₃-pz), 2.44 (3H, s, CH₃-pz), 2.60 (1H, d, CH₂-COO), 2.90 (1H, m, CH₂-S), 3.50 (1H, m, pz-CH₂), 3.75 (1H, d, CH₂-COO), 4.33 (1H, m, CH₂-S), 4.75 (1H, m, pz-CH₂), 6.18 (1H, s, H(4)). ¹³C NMR (CDCl₃): 11.95 (CH₃), 15.60 (CH₃); 34.62 (CH₂); 37.27 (CH₂), 47.04 (CH₂), 108.75(C(4)-pz), 141.83 (C(3/5)-

pz), 154.94 (C(3/5)-pz), 177.30 (C=O), 191.05 (C≡O), 194.03 (C≡O), 197.49 (C≡O). HPLC (gradient 0.1% TFA/methanol): $R_t = 17.47$ min.

4.3. Synthesis of *fac*-[$^{99m}\text{Tc}(\text{CO})_3\{3,5\text{-Me}_2\text{pz}-(\text{CH}_2)_2\text{S-CH}_2\text{-COO}\}$] (**1a**)

In a nitrogen-purged glass vial, 100 μL of 10^{-2} M solution of the compound **1H** was added to 900 μL of a solution of *fac*-[$^{99m}\text{Tc}(\text{OH}_2)_3(\text{CO})_3\text{]}^+$ (1–2 mCi) in NaCl 0.9%. The reaction mixture was incubated at 100 °C for 60 min and then analyzed by HPLC, with a yield >99%. HPLC (gradient 0.1% TFA/methanol): $R_t = 17.56$ min.

4.4. X-ray diffraction analysis

The X-ray diffraction analysis of compound **1** has been performed on a Bruker AXS APEX CCD area detector diffractometer, using graphite monochromated Mo $K\alpha$ radiation (0.71073 Å). Empirical absorption correction was carried out using SADABS [21]. Data collection and data reduction for **1** were done with SMART and SAINT programs [22]. The structure was solved by direct methods with SIR97 [23] and refined by full-matrix least-squares analysis with SHELXL97 [24] using the WINGX [25] suite of programmes. Non-hydrogen atoms were refined with anisotropic thermal parameters whereas H-atoms were placed in idealised positions and allowed to ride on the parent C atom. Molecular graphics were prepared using ORTEP3 [26]. A summary of the crystal data, structure solution and refinement parameters are given in Table 3.

4.5. Challenge experiments against cysteine and histidine

In a nitrogen-purged glass vial were added 900 μL of cysteine and histidine solutions (1.11×10^{-2} – 1.11×10^{-3} M) in PBS (pH 7.4) and 100 μL of the ^{99m}Tc complexes (**1a** or **2a**). The resulting solutions were incubated at 37 °C; aliquots were removed at 1, 2, 4, and 6 h, and analyzed by HPLC.

4.6. Octanol–water partition coefficient

The $\log D_{o/w}$ values of **1a** and **2a** were determined by the multiple back extraction method [13] under physiological conditions (*n*-octanol/0.1 M PBS, pH 7.4). **1a**: $\log D_{o/w} = +1.26 \pm 0.04$; **2a**: $\log P_{o/w} = +1.10 \pm 0.03$.

Table 3
Crystallographic data for complex **1**.

Chemical Formula	$\text{C}_{12}\text{H}_{21}\text{N}_2\text{O}_5\text{SRe}$
Formula weight	491.57
Crystal System	Monoclinic
Space Group	$P2_1/n$
<i>a</i> (Å)	7.5323(3)
<i>b</i> (Å)	18.0823(7)
<i>c</i> (Å)	11.4036(4)
β (°)	100.537(2)
<i>V</i> (Å ³)	1526.99(10)
<i>Z</i>	4
Temperature (K)	293(2)
ρ (calcd.) (g cm ⁻³)	2.138
μ (Mo $K\alpha$) (mm ⁻¹)	8.115
θ range for data collection (°)	2.14–30.50
No. of data	4669
No. of parameters	193
R indices (all data)	$R_1 = 0.0316$ $wR_2 = 0.0491$
R indices [$I > 2\sigma(I)$]	$R_1 = 0.0215$ $wR_2 = 0.0471$
Goodness-of-fit (GOF)	1.032

4.7. Biodistribution studies

Biodistribution studies of complexes **1a** and **2a** were performed using groups of five female CD-1 mice (randomly bred, Charles River) weighing approximately 20–25 g each. Prior to administration, complexes were diluted with PBS pH 7.4. Animals were intravenously injected with 100 μL (2.5–12.5 MBq) of each preparation via the tail vein and were maintained on normal diet ad libitum. At 1 h, and 4 h, mice were sacrificed by cervical dislocation. The administered dose and the radioactivity in the sacrificed animals were measured in a dose calibrator (Aloka, Curimeter IGC-3, Tokyo, Japan). The difference between the radioactivity in the injected and sacrificed animal was assumed to be due to excretion. Blood samples were taken by cardiac puncture at sacrifice. Tissue samples of the main organs were then removed, weighed, and counted in a gamma counter (Berthold, LB2111, Germany). Accumulation of radioactivity in the tissues was calculated and expressed as percentage of the injected dose per gram tissue (% ID/g organ). For blood, bone, and muscle, total activity was calculated assuming that these organs constitute 6%, 10%, and 40% of the total weight, respectively. Urine was also collected at the time of sacrifice.

4.8. Metabolism studies

The *in vivo* stability of **1a** and **2a** was evaluated by urine and murine serum HPLC analysis, using the above referenced experimental conditions. Urine: the urine was collected at sacrifice time and filtered through a Millex GV filter (0.22 μm) before RP-HPLC analysis. Serum: blood collected from mice was immediately centrifuged for 15 min at 3000 rpm at 4 °C, and the serum was separated. Aliquots of 100 μL of serum were treated with 200 μL of ethanol to precipitate the proteins. Samples were centrifuged at 4000 rpm for 15 min, at 4 °C. Supernatant was collected and passed through a Millex GV filter (0.22 μm) prior to RP-HPLC analysis.

4.9. Computational details

All the DFT calculations [11] were performed using the ADF 2006 program [27]. Geometries were optimized without any symmetry constraints using the local functional Vosko, Wilk and Nusair (VWN) [28] in combination with non-local permute (Becke88) [29] and correlation (Perdew86) functional [30]. Relativistic effects were accounted by the scalar correlation ZORA [31] approach. The basis sets consisted of Slater orbitals (STO) with triple ζ to describe the valence orbitals of H (1s); C, O, N (2s, 2p); S (3s,3p); Tc (4s,4p,4d,5s) and Re (4f,5s,5p,5d,6s). These were augmented with a set of two polarization functions: H (2p,3d); C, O, N, S (3d,4f); Re (5p,5f); and Tc (5p,4f). The core electrons were frozen for the atoms C, O, N (1s), S ([1–2]s), Re ([1–4]s, [2–4]p, [3–4]d) and Tc ([1–3]s, [2–3]p, 3d). The solvent effects were included using the COSMO model implemented in the ADF program [17].

The geometry optimizations were done on the available X-ray structures without any simplification. They were used as the basis to create modes for the other complexes. The geometries were optimized again with the solvent, starting from the gas phase geometries.

The nature of the binding interactions was investigated with the energy decomposition analysis (EDA) of ADF [32], originally developed by Morokuma [33] and later modified by Ziegler and Rauk [34]. The interaction energy $\Delta E'$ can be divided into three main components

$$\Delta E' = \Delta E_{\text{Pauli}} + \Delta E_{\text{elec}} + \Delta E_{\text{orb}} \quad (2)$$

ΔE_{elec} gives the electrostatic interaction energy between the ligands and the *fac*-[M(CO)₃]⁺ fragments, which is calculated using the

frozen electron density distribution of the respective ligand and $fac-[M(CO)_3]^+$ in the geometry and electronic reference state of final complexes. ΔE_{Pauli} refers to repulsive interactions associated with the fact that two electrons with the same spin cannot occupy the same region in space. The orbital interaction term, ΔE_{orb} , reflects the covalent interactions between fragments. Further details of the energy partitioning analysis can be found in the literature [32].

Acknowledgments

Carolina Moura thanks FCT for a Ph.D. research grant (SFRH/BD/38469/2007). The authors would like to acknowledge FCT (PPCDT/QUI/59588/2004) and FCT, POCl and FEDER (project POCl/QUI/58925/2004) for financial support.

Appendix A. Supplementary material

CCDC 702244 contains the supplementary crystallographic data for **1**. These data can be obtained free of charge from The Cambridge Crystallographic Data Centre via www.ccdc.cam.ac.uk/data_request/cif. Supplementary data associated with this article can be found, in the online version, at [doi:10.1016/j.jorganchem.2008.11.027](https://doi.org/10.1016/j.jorganchem.2008.11.027).

References

- [1] (a) J.R. Dilworth, S.J. Parrott, *Chem. Soc. Rev.* 27 (1998) 43–55; (b) S.S. Jurisson, J.D. Lydon, *Chem. Rev.* 99 (1999) 2205–2218; (c) S. Liu, *Chem. Soc. Rev.* 33 (2004) 445–461; (d) S. Liu, *Adv. Drug Deliv. Rev.* 60 (2008) 1347–1370.
- [2] F. Tisato, M. Porchia, C. Bolzati, F. Refosco, A. Vittadini, *Coord. Chem. Rev.* 250 (2006) 2034–2045.
- [3] R. Alberto, *Top. Curr. Chem.* 252 (2005) 1–44.
- [4] I. Santos, A. Paulo, J.D.G. Correia, *Top. Curr. Chem.* 252 (2005) 45–84.
- [5] R. Alberto, R. Schibli, A. Egli, A.P. Schubiger, *J. Am. Chem. Soc.* 120 (1998) 7987–7988.
- [6] R. Schibli, R. La Bella, R. Alberto, E. Garcia-Garayoa, K. Ortner, U. Abram, P.A. Schubiger, *Bioconjugate Chem.* 11 (2000) 345–351.
- [7] (a) S.R. Banerjee, M.K. Levalada, N. Lazarova, L. Wei, J.F. Valliant, K.A. Stephenson, J.W. Babich, K.P. Maresca, J. Zubieta, *Inorg. Chem.* 41 (2002) 6417–6425; (b) H.-J. Pietzsch, A. Gupta, M. Reisgys, A. Drews, S. Seifert, R. Syhre, H. Spies, R. Alberto, U. Abram, P.A. Schubiger, B. Johannsen, *Bioconjugate Chem.* 11 (2000) 414–424; (c) D. Kramer, A. Davison, W. Davis, A.G. Jones, *Inorg. Chem.* 41 (2002) 6181–6183; (d) C. Müller, C. Dumas, U. Hoffmann, P.A. Schubiger, R. Schibli, *J. Organomet. Chem.* 689 (2004) 4712–4721; (e) C. Dumas, J. Petrig, L. Frei, B. Spingler, R. Schibli, *Bioconjugate Chem.* 16 (2005) 421–428; (f) C. Müller, P.A. Schubiger, R. Schibli, *Bioconjugate Chem.* 17 (2006) 797–806; (g) A. Chiotellis, C. Tsoukalas, M. Pelecanou, C. Raptopoulou, A. Terzis, M. Papadopoulos, Z. Papadopoulos-Daifoti, I. Pirmettis, *Inorg. Chem.* 47 (2008) 2601–2607.
- [8] (a) S. Alves, A. Paulo, J.D.G. Correia, A. Domingos, I. Santos, *J. Chem. Soc., Dalton Trans.* (2002) 4714–4719; (b) R. Vitor, S. Alves, J.D.G. Correia, A. Paulo, I. Santos, *J. Organomet. Chem.* 689 (2004) 4764–4774; (c) L. Maria, S. Cunha, M. Videira, L. Gano, A. Paulo, I.C. Santos, I. Santos, *Dalton Trans.* (2007) 3010–3019.
- [9] (a) S. Alves, J.D.G. Correia, A. Paulo, L. Gano, J. Smith, I. Santos, *Bioconjugate Chem.* 16 (2005) 438–449; (b) S. Alves, J.D. G. Correia, I. Santos, B. Veerendra, G. Sieckman, T. Hoffman, T. Rold, S.D. Figueroa, L. Retzlöff, J. McCrate, A. Prasanphanich, C. Smith, *Nucl. Med. Biol.* 33 (2006) 625–634; (c) S. Alves, J.D.G. Correia, L. Gano, T.L. Rold, A. Prasanphanich, R. Hauber, M. Rupprich, R. Alberto, C. Decristoforo, I. Santos, C.J. Smith, *Bioconjugate Chem.* 18 (2007) 530–537; (d) C. Decristoforo, A. Rey, J.U. Kuenstler, H.J. Pietzsch, J. D.G. Correia, I. Santos, C.J. Smith, L.B. Faintuch, I. Hernandez-Gonzales, M. Rupprich, R. Alberto, R. Haubner, Q. J. Nucl. Med. Mol. Imaging 51 (2007) 33–41; (e) P.D. Raposinho, C. Xavier, J.D.G. Correia, S. Falcão, P. Gomes, I. Santos, *J. Biol. Inorg. Chem.* 13 (2008) 449–459; (f) P.D. Raposinho, J.D.G. Correia, S. Alves, M.F. Botelho, Ana C. Santos, I. Santos, *Nucl. Med. Biol.* 35 (2008) 91–99.
- [10] C. Fernandes, I.C. Santos, I. Santos, H.-J. Pietzsch, J.-U. Künstler, W. Kraus, A. Rey, N. Margaritis, A. Bourkoulou, A. Chiotellis, M. Paravatou-Petsotas, I. Pirmettis, *Dalton Trans.* (2008) 3215–3225.
- [11] R.G. Parr, W. Young, *Density Functional Theory of Atoms and Molecules*, Oxford University Press, New York, 1989.
- [12] N. Lazarova, S. James, J. Babich, J. Zubieta, *Inorg. Chem. Commun.* 7 (2004) 1023–1026.
- [13] D.E. Troutner, W.A. Volkert, T.J. Hoffman, R.A. Holmes, *Int. J. Appl. Radiat. Isot.* 35 (1984) 467–470.
- [14] M. Lipowska, R. Cini, G. Tamasi, X. Xu, A.T. Taylor, L.G. Marzilli, *Inorg. Chem.* 43 (2004) 7774–7783.
- [15] R. Schibli, N. Marti, P. Maurer, B. Spingler, M.-L. Lehaire, V. Gramlich, C.L. Barnes, *Inorg. Chem.* 44 (2005) 683–690.
- [16] B. Sañ, J. Mertens, F. De Proft, P. Geerlings, *J. Phys. Chem. A* 110 (2006) 9240–9246.
- [17] (a) A. Klamt, G.J. Schuurmann, *J. Chem. Soc., Perkin Trans. 2* (1993) 799–805; (b) A. Klamt, *J. Chem. Phys.* 99 (1995) 2224–2235; (c) C.C. Pye, T. Ziegler, *Theor. Chem. Acc.* 101 (1999) 396–408.
- [18] R.G. Pearson, *J. Am. Chem. Soc.* 85 (1963) 3533–3539.
- [19] T.A. Albright, J.K. Burdett, M.H. Wangbo, *Orbital Interactions in Chemistry*, John Wiley & Sons, New York, 1985.
- [20] P. López, C.G. Seipelt, L. Merkling, J. Sturz, J. Álvarez, A. Dolle, M.D. Zeidler, S. Cerdan, P. Ballesteros, *Bioorg. Med. Chem.* 7 (1999) 517–527.
- [21] SADABS: Area-Detector Absorption Correction, Bruker AXS Inc., Madison, WI, 2004.
- [22] SAINT: Area-Detector Integration Software (Version7.23), Bruker AXS Inc., Madison, WI, 2004.
- [23] A. Altomare, M.C. Burla, M. Camalli, G. Cascarano, G. Giacovazzo, A. Guagliardi, A.G.G. Moliterni, G. Polidoro, R. Spagna, *J. Appl. Crystallogr.* 32 (1999) 115.
- [24] G.M. Sheldrick, SHELXL-97: Program for the Refinement of Crystal Structure, University of Göttingen, Germany, 1997.
- [25] L.J. Farrugia, *J. Appl. Crystallogr.* 32 (1999) 837–838.
- [26] L.J. Farrugia, ORTEP-3, *J. Appl. Crystallogr.* 30 (1997) 565.
- [27] (a) G. Velde, F.M. Bickelhaupt, S.J.A. van Gisbergen, C.F. Gerra, J.G. Snijders, T. Ziegler, *J. Comput. Chem.* 22 (2001) 931–967; (b) C.F. Guerra, J.G. Snijders, G. Velde, E.J. Baerends, *Theor. Chem. Acc.* 99 (1998) 391–403; (c) ADF2006.01, SCM, Theoretical Chemistry, Vrije Universiteit, Amsterdam, The Netherlands, <<http://www.scm.com>>.
- [28] S.H. Vosko, L. Wilk, M. Nusair, *Can. J. Phys.* 58 (1980) 1200–1211.
- [29] A.D. Becke, *J. Chem. Phys.* 88 (1988) 1053–1062.
- [30] J.P. Perdew, J.A. Chevary, S.H. Vosko, K.A. Jackson, M.R. Pederson, D.J. Singh, C. Fiolhais, *Phys. Rev. B* 46 (1992) 6671–6687.
- [31] (a) C. Chang, M. Pelissier, P. Durand, *Phys. Scripta* 34 (1986) 394; (b) J.-L. Heully, I. Lindgren, E. Lindroth, S. Lundquist, A.-M. Martensson-Pendrill, *J. Phys. B* 19 (1986) 2799; (c) E. van Lenthe, E.J. Baerends, J.G. Snijders, *J. Chem. Phys.* 99 (1993) 4597; (d) J.G. van Lenthe, E.J. Baerends, J.G. Snijders, *J. Chem. Phys.* 105 (1996) 6505; (e) E. van Lenthe, R. van Leeuwen, E.J. Baerends, J.G. Snijders, *Int. J. Quantum Chem.* 57 (1996) 281.
- [32] (a) F.M. Bickelhaupt, E.J. Baerends, in: K.B. Lipkowitz, D.B. Boyd (Eds.), *Reviews in Computational Chemistry*, vol. 15, Wiley-VCH, New York, 2000, p. 1; (b) M. Lein, G. Frenking, in: C.E. Dykstra, G. Frenking, K.S. Kim, G.E. Scuseria (Eds.), *Theory and Applications of Computational Chemistry, the First 40 Years*, Elsevier, Amsterdam, 2005, p. 367; (c) G. Frenking, K. Wichmann, N. Fröhlich, C. Loschen, M. Lein, J. Frunzke, V.M. Rayón, *Coord. Chem. Rev.* 238–239 (2003) 55.
- [33] (a) K.J. Morokuma, *Chem. Phys.* 55 (1971) 1236; (b) K. Kitaura, K. Morokuma, *Int. J. Quantum Chem.* 10 (1976) 325.
- [34] (a) T. Ziegler, A. Rauk, *Theor. Chim. Acta* 46 (1977) 1; (b) T. Ziegler, A. Rauk, *Inorg. Chem.* 18 (1979) 1755; (c) T. Ziegler, A. Rauk, *Inorg. Chem.* 18 (1979) 1558.